

Capturing patterns of variation unique to a specific dataset

Robin Tu¹, Alexander H. Foss², and Sihai Dave Zhao¹

¹Department of Statistics, University of Illinois at Urbana-Champaign,
Champaign, IL

²Statistical Sciences, Sandia National Laboratories, Albuquerque, NM

January 12, 2021

1 Introduction

Capturing patterns of variation present in a dataset is an important step in exploratory data analysis and unsupervised learning. Popular methods include principal component analysis (PCA) [11], nonnegative matrix factorization [15], projection pursuit [10], and independent component analysis [8]. Frequently, however, many of the identified patterns may actually arise from systematic or technical variation, for example batch effects, that are not of substantive interest.

New approaches are necessary for capturing meaningful patterns of variation. A popular approach is to contrast a target dataset of interest with a carefully chosen background dataset that represents unwanted or uninteresting variation. Patterns of variation unique to the target, and not present in the background, are more likely to be substantively meaningful. For example, in Section 2.1, we analyze proteomics data from normal and trisomic mice that have undergone Context Shock treatment and/or drug therapy. One goal is to identify patterns uniquely associated with normal mice. However, the dominant modes of variation in the dataset arise from the Context Shock treatment and the trisomic gene, which are not of interest. Therefore, we contrast the data with a background dataset of proteomics data from Context Shock-treated and drug-treated trisomic mice. As a result, the remaining patterns of variation unique to the target dataset reveal features specific to normal mice.

This approach was first introduced by Abid et al. [1], who proposed contrastive principal components analysis (cPCA). While standard PCA identifies directions of variation that explain the most variation in the target dataset, cPCA seeks directions that explain more variation in the target than in the background. The most important patterns are those corresponding to the largest gap between the two datasets. Salloum and Kuo [19] later introduced cPCA++, which maximizes the ratio, rather than the difference, of the variance explained by the target and background. Boileau et al. [4] described sparse cPCA, which

seeks maximally contrastive patterns of variation that can be characterized using a parsimonious set of features. Other types of contrastive implementations include latent models [20] and autoencoders [2].

There are two main issues with existing contrastive methods. First, a major disadvantage is that they cannot accommodate multiple background datasets. Using multiple backgrounds allows researchers to better hone in on the unique variation of interest by removing multiple types or sources of unwanted variation. For example, in the emotion analysis in Section 2.2, where we seek to uncover facial features characterizing the expression of “afraid”, the dataset we use also contains background images from six other emotions. If we can simultaneously contrast the target data with multiple other background emotions, we will be able to identify more refined and distinctive patterns of variation characterizing “afraid”. Naively applying existing methods by pooling the different emotions into a single background dataset is sub-optimal, as variation in the pooled data may not be representative of variation in any of the individual datasets.

The second disadvantage of existing contrastive methods is that they typically require one or more tuning parameters. For example, cPCA requires the user to specify how much to penalize patterns that explain a large amount of variation in the background data. It is not clear in general how to choose these tuning parameters objectively.

We propose Unique Component Analysis (UCA), which addresses both of these issues. Not only can UCA contrast a target dataset against multiple backgrounds, but it also does not require any tuning parameters. UCA finds directions of variation that maximize the explained variation in the target under a constraint on the amount of variation they can explain in each of the backgrounds. With a single background, UCA is equivalent to cPCA but with an automatically selected tuning parameter. We show that UCA achieves similar results as cPCA and cPCA++ with a single background and that it can outperform them when using multiple backgrounds. We also develop computationally scalable algorithms for application to experiments with large numbers of measured features.

2 Results

2.1 Discovering subgroups in protein expression data

We applied UCA to mouse proteomics data, which were also used by Abid et al. [1] to illustrate cPCA performance. The study measured levels of 76 proteins in 1080 normal and trisomic (Down Syndrome) mice receiving various combinations of learning therapies (Context Shock vs. Shock Context) and drug (memantine vs. saline) [3, 14, 1]. Normal mice exposed to Context Shock will first be exposed to novel context then shocked, and learn to associate novel contexts with adverse stimulus; trisomic mice will not learn this association. Under the Shock Context treatment, mice are first shocked then exposed to novel context, resulting in normal and trisomic mice not associating the environment with adverse stimulus. The goal of the experiment was to assess whether memantine improved learning ability in trisomic mice and to identify subsets of protein that may be involved in this process.

We first replicate the analysis by Abid et al. [1]. We want to extract patterns of variation in protein levels that can help discriminate normal from trisomic mice. Our target dataset

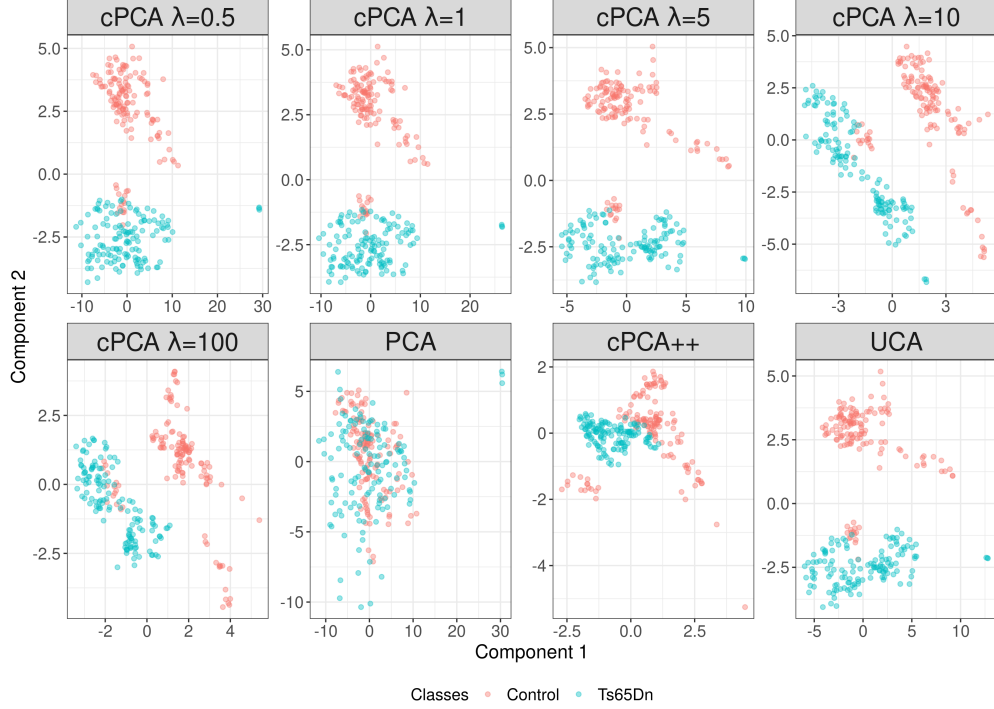


Figure 1: Mouse Protein Expression: Down Syndrome (Ts65Dn) separability of saline injected mice which were shocked before getting environmental context (Shock Context). Both normal and trisomic mice receiving Shock Context treatment do not associate novel environments with adverse stimulus. Down Syndrome and control mice were unseparable using PCA alone but is easily separable by cPCA at all values of the contrastive parameter λ . The mice are also easily separable by cPCA++ and UCA.

consisted of protein data from Shock Context mice given saline. However, natural variation, arising from factors such as age and gender, may dominate this dataset and obscure the variation of interest due to trisomy. To remove this natural variation, we contrasted the target data with a background dataset consisting of normal Context Shocked mice who had been given saline. As natural variation is likely present in both the target and the background, patterns that explaining variation in the target but not the background may be more likely to be related to trisomy.

Figure 1 shows the data projected to the first two components identified by PCA, cPCA, cPCA++, and UCA. Normal and trisomic mice are not well-separated in the PCA results, showing that dominant variation in the target data indeed does not stem from trisomy. In contrast, the two mouse groups are much more clearly separated in the cPCA results. While this separation is noticeable for each of the tuning parameter values we tried, the actual projected data can vary considerably, and the optimal tuning parameter value remains unclear. cPCA++, which does not require specifying tuning parameter here because the number of samples exceeds the number of features, shows better separation than PCA but does not perform as well as cPCA. UCA performs as well as cPCA but without requiring a tuning parameter.

We next repeat the same analysis, but this time using Context Shocked mice given saline

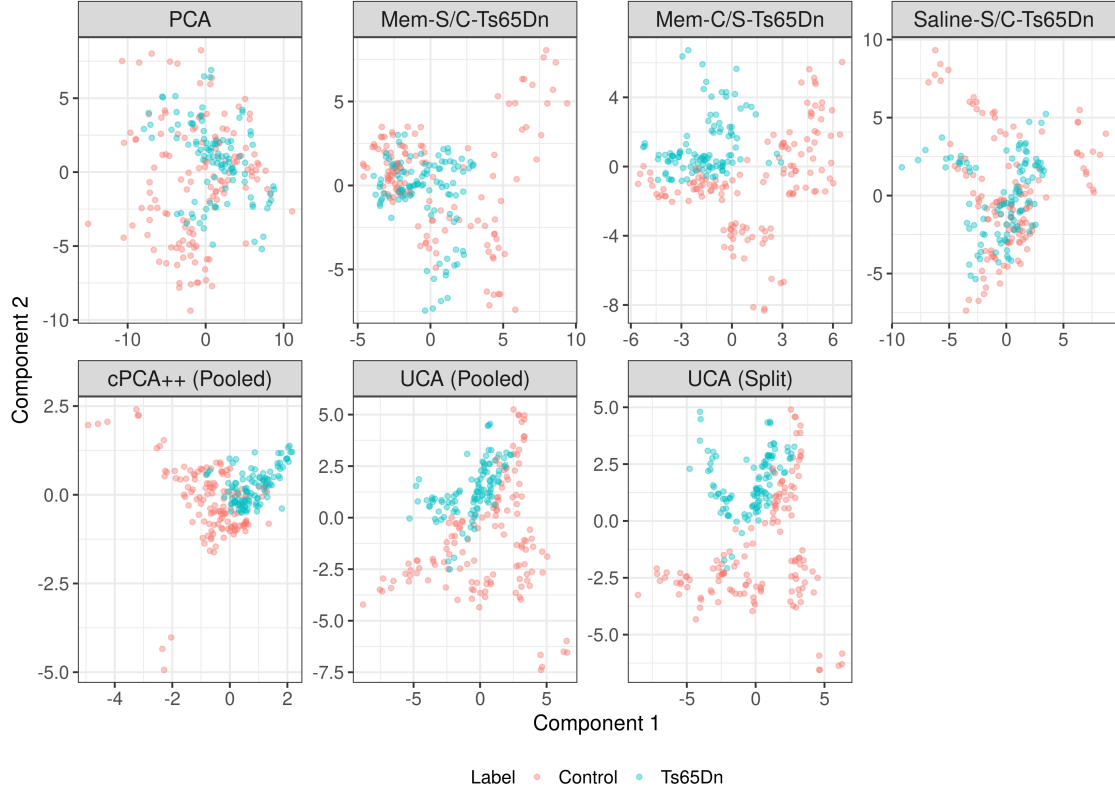


Figure 2: Mouse Protein Expression: Separability of normal and trisomic Context Shocked mice injected with saline. Background datasets: Shock Context trisomic mice injected with memantine (Mem-S/C-Ts65Dn), Context Shock trisomic mice injected with memantine (Mem-C/S-Ts65Dn), and Shock Context trisomic mice injected with saline (Saline-S/C-Ts65Dn). Pooled: all background datasets are pooled into one background. Split: UCA using multiple separate individual backgrounds.

as our target dataset. Abid et al. [1] did not consider this analysis, where separating normal and trisomic Context Shocked mice proves to be a much more challenging problem. Figure 2 shows that normal and trisomic mice are again not well-separated by the first two components learned by PCA. Here we extract patterns of variation unique to normal mice and so applied UCA using three trisomic mouse datasets as backgrounds.

The results show that a single background dataset alone cannot separate normal and trisomic mice well. Pooling the three individual backgrounds together achieves slightly better separability compared to some of the individual backgrounds. However, natively contrasting multiple backgrounds simultaneously without pooling allows our proposed UCA to remove variability specific to each background and results in the best separability.

2.2 Discovering eigenfaces of emotion

We further illustrate the advantages of contrasting multiple background datasets with UCA using the Karolinska Directed Emotional Faces (KDEF) [7], which captured images of seven

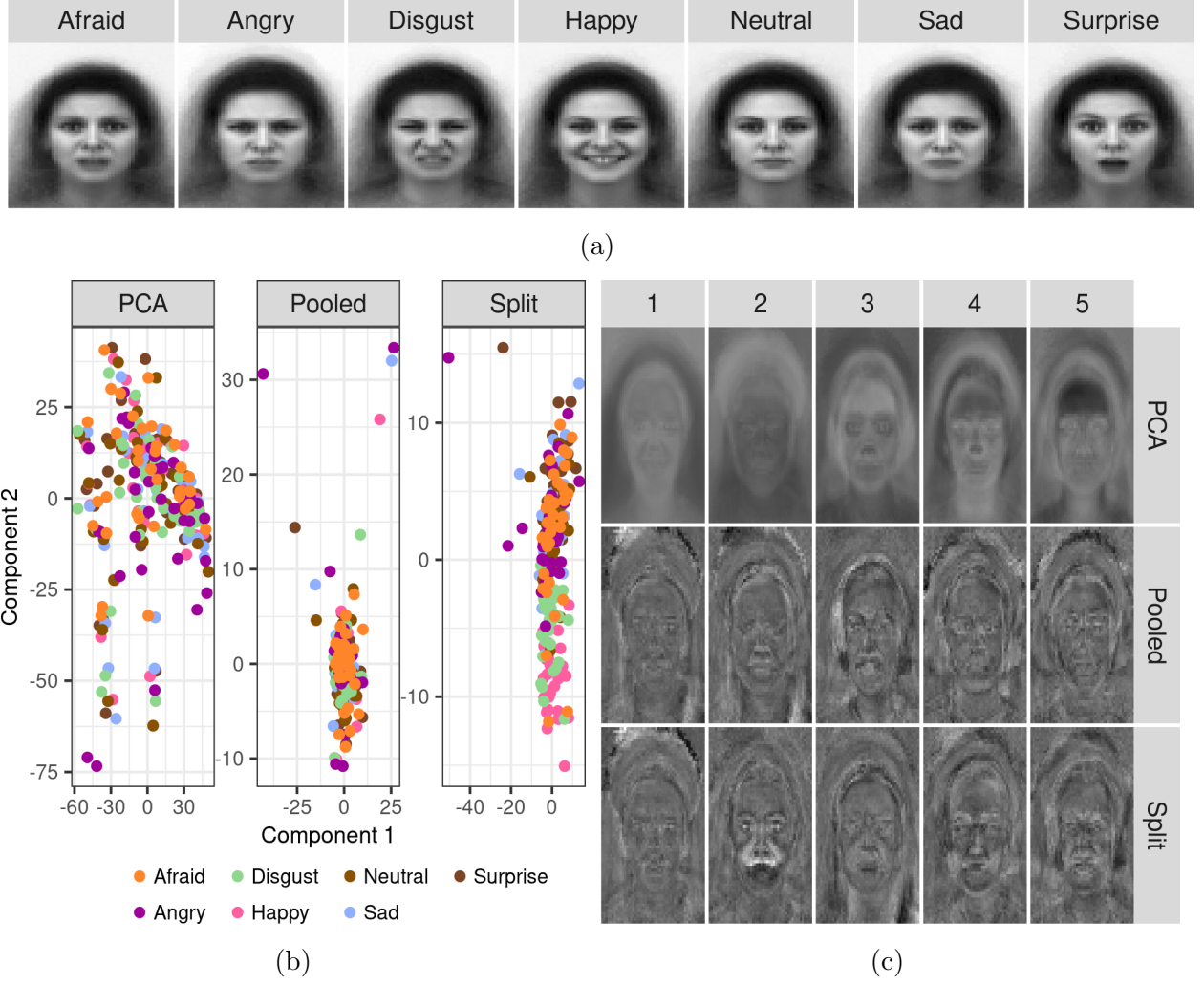


Figure 3: Results of analysis of KDEF faces. (a) Each emotion averaged over all female actors. (b) Faces projected onto the first two components found by PCA, UCA with a pooled background, and UCA using multiple backgrounds. (c) Top 5 eigenfaces of female emotions produced by different analyses.

emotions from five different angles from 70 amateur actors in either a practice or final session. Figure 3a presents averaged images of each emotion calculated from all female actors in their final session.

We focus on uncovering variation unique to the “afraid” emotion using all final session pictures from every emotion from female actors. Since this target contains six other emotions, standard PCA will not provide variation unique to “afraid”. Instead, we leverage images from the practice session to serve as background data. We construct six separate backgrounds, corresponding to the six other emotions, and contrast out their variation using UCA. For comparison, we also pooled these images together into a single background dataset and performed UCA using the pooled background.

Figure 3b projects the target data onto the first two directions of variation calculated using each method. The emotions are entirely intermixed when projected onto components

produced by PCA and by UCA using a single pooled background. In contrast, the emotions are much more separable when using UCA with multiple separate backgrounds. In particular, “afraid” faces are very separate from the “disgust” and “happy” faces. This indicates that UCA with multiple backgrounds can identify patterns of variation that can distinguish “afraid” from the other emotions.

Figure 3c shows visualizes the top five directions of variation produced by each method as faces. These are called eigenfaces, and this visualization technique is useful for interpreting the top components as facial features [21]. PCA eigenfaces generally represent features common to all the emotions. UCA eigenfaces using a pooled background seem to highlight the eyebrows and upper lips, though it is difficult to discern. On the other hand, eigenfaces produced using UCA using multiple separate backgrounds highlight eyebrows, eyes, nostrils, and nasolabial folds. These are especially clear in the second eigenface and accord with intuition about which features would likely be most useful in distinguishing “afraid” from other emotions.

3 Discussion

In many data analytics settings, we are interested in removing uninteresting variation that contaminate the data of interest. Here we proposed UCA, a tuning-free contrastive learning method that can accommodate multiple background datasets and have shown its usefulness in several examples. We showed in analyses of mouse proteomics data and facial image data that UCA performs as well as cPCA when used with a single background dataset but can have dramatically better performance when used with multiple separate backgrounds.

UCA is computationally fast and easily extensible to high-dimensional data because it does not require constructing nor storing a large covariance matrices (see Methods). Further, no additional post-hoc clustering method is necessary to choose the appropriate tuning parameter.

Like cPCA, the choice of background(s) still play a pivotal role in the directions found by UCA. For background data that is already accounted for by other background data, the algorithm will ignore similar information and only weigh additional new information. In the event of identical backgrounds, only one background will be considered. This can be avoided apriori by stacking data from the same experiments and creating a joint background.

Similar to regression, switching target and background covariance matrices will not result in the same solution. UCA finds variation in the target data not present in the background data.

We have released the code for UCA as an R package, along with documentation and examples exhibited in this paper.

4 Method

4.1 Contrastive principal components analysis

We first briefly review cPCA [1]. Let A denoted the $p \times p$ sample covariance matrix constructed from target data $X_{n_x \times p}$ and B denote the $p \times p$ sample background covariance constructed

from background data $Y_{n_y \times p}$. For some parameter λ , cPCA seeks the eigenvectors, $v_\lambda \in \mathbb{R}^p$, which account for large variation in the target data Y and small variation in the background data X where $\|v\|_2 = 1$. Specifically:

$$v_\lambda = \arg \max_{v \in \mathbb{R}^p} (v^T A v - \lambda v^T B v) \text{ subject to } v^\top v = 1$$

For a given λ , the direction is simply the eigenvector of the weighted difference between covariance matrices where v maximize the variation in A while constraining variation in B . The tuning parameter λ measures how much to penalize the background data covariance. When $\lambda = 0$, background variation is not considered, therefore cPCA reduces to PCA. As λ increases, the relative background variation becomes more dominant, causing v_λ to focus on directions which minimize background variation rather than maximizing the target. For very large values of λ , v_λ is equivalent to PCA after projecting the target data onto the nullspace of the background data. The authors of cPCA suggested that λ be chosen using spectral clustering via a parameter sweep of logarithmically spaced candidate values.

We can rewrite the cPCA problem as a Rayleigh quotient

$$v_\lambda = \arg \max_{v \in \mathbb{R}^p} \frac{v^T (A - \lambda B) v}{v^T I v}$$

and observe that the variability in X and Y are measured relative to the identity matrix.

4.2 cPCA++

Salloum and Kuo [19] arrived at a tuning free contrastive method, cPCA++, where they seek to maximize the ratio, rather than the difference, of the variance explained in the target to the variance explained in the background. Using similar notation as above where A denotes the target sample covariance matrix and B denotes the background sample covariance matrix, cPCA++ seeks to maximize the Rayleigh quotient:

$$v = \arg \max_{v \in \mathbb{R}^p} \frac{v^T A v}{v^T B v}$$

While maximizing the relative variability between A and B is tuning free, the solution involves a matrix inversion, which may not be feasible in high-dimensional applications like genomics where the inverse may not exist. Furthermore, there is no clear path to extend this problem to multiple backgrounds. For clarity, We rewrite the cPCA++ objective function to it's primal form[12]:

$$\max_{v \in \mathbb{R}^p} v^T A v \text{ subject to } v^T B v = 1$$

4.3 Unique Component Analysis

We introduce the Unique Component Analysis (UCA) framework which combines both cPCA and cPCA++ to objectively solve for the contrastive parameter, λ and resulting directions of variation using lagrangians. UCA works by joining the constraints of $v^T v = 1$ from cPCA

and $v^T B v = 1$ from cPCA++. For a single background covariance matrix UCA solves the primal problem:

$$\begin{aligned} & \max_{v \in \mathbb{R}^p} v^T A v \\ & \text{subject to } v^T v = 1, \quad v^T B v \leq 1 \end{aligned} \tag{1}$$

Since our primal problem is quadratic, strong duality requires satisfying Slater's condition[5] (See Appendix B1). To achieve strong duality, we require the smallest eigenvalue of B to be less than 1, $\lambda_{\min}(B) = \min_v \frac{v^T B v}{v^T v} < 1$. This requirement follows naturally for covariance matrices formed from standardized data due to the ordering of eigenvalues and:

$$\text{tr}(B) = \sum_{i=1}^p \lambda_i = n$$

implies $\lambda_{\min}(B) \leq 1$, with equality if $B = I_p$. For covariance matrices formed from unstandardized data, our assumption is the same as $\dim(B) < p$, the dimensionality of B is smaller than p . With strong duality, we solve 1 by maximizing the dual function, $g(\lambda)$ of the Lagrangians \mathcal{L} :

$$\begin{aligned} \max_{\lambda \geq 0} g(\lambda) &= \max_{\lambda \geq 0} \max_{v \in \mathbb{R}^P} \mathcal{L}(v, \lambda) \\ &= \max_{\lambda \geq 0} \max_{v \in \mathbb{R}^P} (v^T A v - \lambda (v^T B v - 1)) \\ &= \max_{\lambda \geq 0} \max_{v \in \mathbb{R}^P} (v^T (A - \lambda B) v + \lambda) \\ &= \max_{\lambda \geq 0} (\lambda_{\max}(A - \lambda B) + \lambda) \\ &= \max_{\lambda \geq 0} (v_{\lambda}^T (A - \lambda B) v_{\lambda} + \lambda) \end{aligned} \tag{2}$$

where λ is the Lagrange multiplier associated with the constraint $v^T B v \leq 1$, $\lambda_{\max}(A - \lambda B)$ is the largest eigenvalue associated with $A - \lambda B$, and v_{λ} is the corresponding eigenvector. Although the primal problem has two constraints, $v^T v = I$ is enforced through eigendecomposition when solving for the largest eigenvalue λ_{\max} .

Since the dual function is concave and a solution necessarily exists, we maximize the dual function (2) by taking the derivative with respect to λ and set the derivative equal to zero:

$$\begin{aligned} \frac{\partial}{\partial \lambda} g(\lambda) &= \frac{\partial}{\partial \lambda} (v_{\lambda}^T (A - \lambda B) v_{\lambda} + \lambda) \\ &\Leftrightarrow \frac{\partial}{\partial \lambda} (-\lambda (v_{\lambda}^T B v_{\lambda}) + \lambda) \\ &= 1 - v_{\lambda}^T B v_{\lambda} = 0 \end{aligned} \tag{3}$$

We use an iterative algorithm (L-BFGS-B) [6] to search for Lagrange multiplier λ such that the associated eigenvectors v_{λ} satisfies equation 3. Due to strong duality, the resulting v_{λ} also solves the primal problem. We see that combining the two constraints allows us a

natural way to solve for the contrastive parameter λ in cPCA when only one background is used.

Similarly, for multiple backgrounds, again let the A be the target $p \times p$ covariance matrix and B_1, \dots, B_m now be the m background $p \times p$ covariance matrices constructed from a $n_y \times p$ dimensional Y data matrix and corresponding $(n_{x_1} \times p), \dots, (n_{x_m} \times p)$ dimensional X_1, \dots, X_m background data matrices. We add additional constraints $v^T B_j v \leq 1$ to our optimization problem for each background $j = 1, \dots, m$. Specifically, for multiple backgrounds, the primal problem becomes

$$\begin{aligned} & \max_{v \in \mathbb{R}^p} v^T A v \\ & \text{subject to } v^T v = 1, \quad v^T B_1 v \leq 1, \dots, v^T B_m v \leq 1 \end{aligned} \quad (4)$$

Maximizing the corresponding dual function $g(\lambda_1, \dots, \lambda_m)$:

$$\begin{aligned} \max_{\lambda_1, \dots, \lambda_m \geq 0} g(\lambda_1, \dots, \lambda_m) &= \max_{\lambda_1, \dots, \lambda_m \geq 0} \max_{v \in \mathbb{R}^p} \mathcal{L}(v, \lambda_1, \dots, \lambda_m) \\ &= \max_{\lambda_1, \dots, \lambda_m \geq 0} \max_{v \in \mathbb{R}^p} \left(v^T \left(A - \sum_{j=1}^m \lambda_j B_j \right) v + \sum_{j=1}^m \lambda_j \right) \\ &= \max_{\lambda_1, \dots, \lambda_m \geq 0} \left(\lambda_{\max} \left(A - \sum_{j=1}^m \lambda_j B_j \right) + \sum_{j=1}^m \lambda_j \right) \end{aligned} \quad (5)$$

For background $j \in 1, \dots, m$, we can solve for the j th Lagrange multiplier in equation 5 similarly by taking the partial derivative and setting to zero:

$$\begin{aligned} \frac{\partial}{\partial \lambda_j} \left(\lambda_{\max} \left(A - \sum_{j=1}^m \lambda_j B_j \right) + \sum_{j=1}^m \lambda_j \right) &= \frac{\partial}{\partial \lambda_j} v_{\lambda}^T \left(A - \sum_{j=1}^m \lambda_j B_j \right) v_{\lambda} + \sum_{j=1}^m \lambda_j \\ &\Leftrightarrow \frac{\partial}{\partial \lambda_j} (v_{\lambda}^T (A - \lambda_j B_j) v_{\lambda} + \lambda_j) \\ &\Leftrightarrow \frac{\partial}{\partial \lambda_j} (-\lambda_j v_{\lambda}^T B_j v_{\lambda} + \lambda_j) \\ &= 1 - v_{\lambda_j}^T B_j v_{\lambda_j} = 0 \end{aligned} \quad (6)$$

To solve this multiple background dataset problem we propose a coordinate descent algorithm that utilizes the single background dataset L-BFGS-B [6] algorithm iteratively. For m background datasets, on the q^{th} iteration, let $A_{(j)}^*$ be the variation in A after excluding background variation that is not B_j :

$$A_{(j)}^* = A - \sum_{i=1}^{j-1} \lambda_i^{(q+1)} B_i - \sum_{i=j+1}^m \lambda_i^{(q)} B_i$$

to solve for j^{th} of the m Lagrange multipliers, we use Algorithm 1.

Algorithm 1: coordinate descent algorithm

Inputs: m centered background data X_1, \dots, X_m , centered Target data Y , k number of components;

Initialize $\lambda_1^{(0)}, \dots, \lambda_m^{(0)}$, ϵ ;

Compute the emperical covariance matrices:

$$A = \frac{1}{n_y} Y^T Y, \quad B_1 = \frac{1}{n_{x_1}} X_1^T X_1, \quad \dots, \quad B_m = \frac{1}{n_{x_m}} X_m^T X_m$$

while $l^{(q+1)} - l^{(q)} > \epsilon$ **do**

for $j = 1 : m$ **do**

 Solve for $\lambda_j^{(q+1)}$ via L-BFGS-B, corresponding to the largest eigenvalue of

$$C_{\lambda_j} = A_{(j)}^* - \lambda_j^{(q+1)} B_j$$

 After iterating through m Lagrange multipliers, calculate value of Lagrangian

$$l^{(q+1)} = \lambda_{max} \left(A - \sum_{j=1}^m \lambda_j^{(q+1)} B_j \right) + \sum_{j=1}^m \lambda_j^{(q+1)}$$

 Compute

$$C_{\lambda_1, \dots, \lambda_m} = A - \sum_{j=1}^m \lambda_j B_j$$

 Find $V_k \in \mathbb{R}^k$, spanned by the top k eigenvectors of $C_{\lambda_1, \dots, \lambda_k}$;

Return: V_k

4.4 Extension to High Dimensional Data:

Under the high-dimensional situation, where the number of variables p far exceeds the number of samples n , constructing the covariance matrix and using eigendecomposition to find the top eigenvectors becomes computationally expensive. To avoid the intermediary of creating and storing a large $p \times p$ covariance matrix, singular-value decomposition (SVD) of the data matrix is frequently used to find the top eigenvalue/eigenvectors of its covariance. To extend our method to high-dimensional data, we analogously avoid the traditional eigendecomposition method of finding eigenvalue/eigenvectors of the covariance matrix that current methods employ. We introduce the Product SVD method to exploit the structure of how the contrastive covariance matrices are formed and employ SVD of a product of matrices to quickly find our top eigenvalue. Breaking the problem down in this way considerably speeds up our L-BFGS-B algorithm, and allows us to run UCA even in the high-dimensional setting.

For a single background, let the $p \times p$ covariance matrices A be the target covariance matrix and B be the background covariance matrix. A and B are formed from corresponding

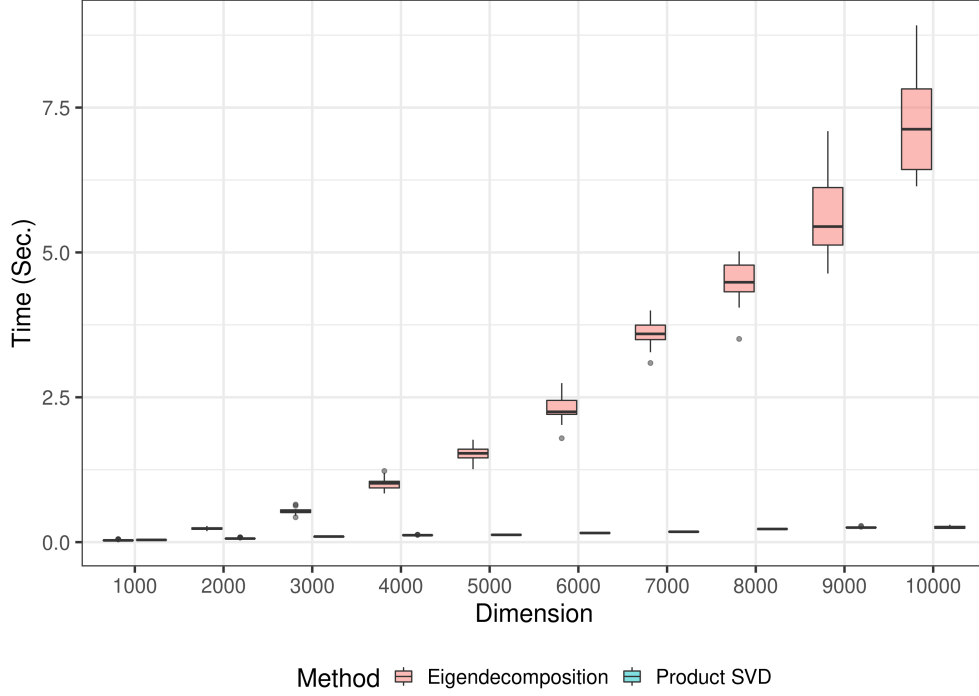


Figure 4: UCA and cPCA implementation using Product SVD vs. eigendecomposition for high-dimensional data: 25 random $100 \times p$ target and background matrices are generated from a standard normal distribution and where p , the dimension varied from 1,000 to 10,000 in steps of 1,000. Box plots of time (in seconds) is plotted for both eigendecomposition and the product SVD method. For small p , there is a negligible difference between the methods. However, as dimension p increases, the Product SVD is significantly faster.

centered $n_y \times p$ target data matrix Y , and centered $n_x \times p$ background data matrix X . We can write the difference of the covariance matrices $A - \lambda B$ as a product of a $p \times (n_y + n_x)$ dimensional left matrix, L , and a $(n_y + n_x) \times p$ dimensional right matrix, R as seen in equation 7:

$$\begin{aligned}
 C_\lambda &= A - \lambda B \\
 &= \frac{1}{n_y} Y^T Y - \frac{\lambda}{n_x} X^T X \\
 &= \underbrace{\left[\frac{1}{\sqrt{n_y}} Y^T, -\frac{\lambda}{\sqrt{n_x}} X^T \right]}_L \underbrace{\begin{bmatrix} \frac{1}{\sqrt{n_y}} Y \\ \frac{1}{\sqrt{n_x}} X \end{bmatrix}}_R
 \end{aligned} \tag{7}$$

With this formulation, we can follow the steps in Golub et al. [13], and find the singular values and vectors of C_λ using a sequence of SVD and QR decompositions operating on the left and right matrices. Since singular values and eigenvalues coincide in square matrices, we use the singular vectors, U , to find the largest eigenvalues by sorting the diagonal of $ULRU^T$. We describe the Product SVD Method in algorithm 2, which can directly replace the more computationally expensive eigendecomposition in high dimensions.

Algorithm 2: Product SVD Method to calculate the largest Eigenvalue of C_λ

Input: Centered background matrix X , centered target matrix Y , and λ ;

- 1 Construct $L = \left[\frac{1}{\sqrt{n_y}} Y^T, -\frac{\lambda}{\sqrt{n_x}} X^T \right]$, $R = \begin{bmatrix} \frac{1}{\sqrt{n_y}} Y \\ \frac{1}{\sqrt{n_x}} X \end{bmatrix}$;
 - 2 SVD the right matrix, $R = U_R S_R V_R^T$;
 - 3 QR decompose LU_R into $Q_{LU_R} R_{LU_R}$;
 - 4 SVD the product of R_{LU_R} (step 3) and S_R (step 2), $R_{LU_R} S_R = E D F^T$;
 - 5 The singular vectors of C_λ is the product of Q (step 3) and E (step 4),
 $U_{C_\lambda} = Q_{LU_R} E$;
 - 6 Find the largest eigenvalues of C_λ by sorting the diagonal of D_{C_λ} , where
 $D_{C_\lambda} = U_{C_\lambda} C_\lambda U_{C_\lambda}^T$;
- Output:** $\lambda_{\max}(C_\lambda)$
-

Similarly, for multiple backgrounds, again let the A be the target $p \times p$ covariance matrix and B_1, \dots, B_m be the m background $p \times p$ covariance matrices constructed from a $n_y \times p$ dimensional Y data matrix and corresponding $(n_{x_1} \times p), \dots, (n_{x_m} \times p)$ dimensional X_1, \dots, X_m background data matrices.

We can construct $C_{\lambda_1, \dots, \lambda_m} = A - \sum_{j=1}^m \lambda_j B_j$ analogously by appending the additional datasets to the left and right matrices:

$$\begin{aligned}
 C_{\lambda_1, \dots, \lambda_m} &= A - \sum_{j=1}^m \lambda_j B_j \\
 &= \frac{1}{n_y} Y^T Y - \sum_{j=1}^m \frac{\lambda_j}{n_{x_j}} X_j^T X_j \\
 &= \underbrace{\left[\frac{1}{\sqrt{n_y}} Y^T, -\frac{\lambda_1}{\sqrt{n_{x_1}}} X_1^T, \dots, -\frac{\lambda_m}{\sqrt{n_{x_m}}} X_m^T \right]}_L \underbrace{\begin{bmatrix} \frac{1}{\sqrt{n_y}} Y \\ \frac{1}{\sqrt{n_{x_1}}} X_1 \\ \vdots \\ \frac{1}{\sqrt{n_{x_m}}} X_m \end{bmatrix}}_R
 \end{aligned} \tag{8}$$

Using the coordinate descent (algorithm 1) to solve for each λ_j prescribed above, we can substitute the eigendecomposition of the covariance matrix, C_{λ_j} with the Product SVD method (algorithm 2) using L and R defined in equation 8.

The Product SVD method is advantageous in high-dimensions because it never explicitly operates on the entire $p \times p$ covariance matrix. Not only is our method more memory efficient, scaling with $n \times p$ bytes rather than p^2 bytes, but our method is also computationally more efficient at finding the largest eigenvalue/eigenvector as operating SVD and QR decomposition on either the left or right matrices is faster than directly operating eigendecomposition on the covariance matrix. In the single background scenario, λ only appears in L . Thus since, R doesn't change, we can pre-compute the SVD of R , and only update L when solving for λ_{\max} . Similarly, in the multi-background scenario, rather than modifying

A^* in the original coordinate descent algorithm, this method allows us to only modify the $j + 1$ element of the left data matrix, L . The SVD of the right matrix, R , only needs to be computed once in our coordinate descent. Furthermore, at each step within the coordinate descent only step 3 and 4, the SVD and QR, are computed, and are done on matrices with dimensions much smaller than $p \times p$.

To demonstrate the speed improvements of the Product SVD method compared to the current fastest implementations of eigendecomposition in high-dimensions, we conduct a simulation study with 25 sample $100 \times p$ target and background data matrices generated from a standard Normal distribution with p varying from 1,000 to 10,000 in steps of 1,000. To ensure a fair comparison, we leverage C++ in both implementations using a custom RcppArmadillo [9] function for the Product SVD method and the RSpectra package (0.16-0) [17] for the eigendecomposition method; RSpectra being a package designed for large-scale eigendecompositions based off the C++ Spectra library. We use the microbenchmark package [16] to ensure accurate timings. Our benchmark does not take into account the additional cost of forming the $p \times p$ covariance matrices, which would only exacerbate the difference between the two methods in real world applications.

Figure 4 show box plots of time (in seconds) versus the dimension, p , colored by method, summarizes the results of the simulation study. As dimension p increases, the computational time of our Product SVD method increases much slower than the current eigendecomposition implementations. It should be mentioned that for $p < 1000$ the Product SVD method is slower due to overhead of additional computation on small matrices. In general, for low-dimensional settings where $n \geq p$, the Product SVD will be negligibly slower because of the additional QR, SVD, matrix products, and sort computations.

All computations in this paper were done with R 3.6.3 [18] on an AMD Ryzen 1700X 3.7 GHz processor and 64GB 3000 mhz DDR4 RAM, utilizing the Intel MKL libraries.

4.5 Code Availability

We have released a R implementation of <https://github.com/rtud2/Residual-Dimension-Reduction>. We have implemented both Product SVD on the data matrix and eigendecomposition on the contrastive covariance matrix and allow the background to take either a single background or a list of backgrounds. The GitHub repository also includes R markdown and datasets that reproduce most of the figures in this paper and in the Supplementary.

4.6 Data availability

Datasets that have been used to evaluate UCA in this paper are publicly available from the authors of the original studies. The mouse proteomics data are available from the UC Irvine Machine Learning Repository <https://archive.ics.uci.edu/ml/datasets/Mice+Protein+Expression> [14] and the Karolinska Directed Emotional Faces (KDEF) are available from <https://www.kdef.se/> [7].

References

- [1] Abubakar Abid, Martin J. Zhang, Vivek K. Bagaria, and James Zou. Exploring patterns enriched in a dataset with contrastive principal component analysis. *Nature Communications*, 9:2134, 05 2018.
- [2] Abubakar Abid and James Zou. Contrastive variational autoencoder enhances salient features, 2019.
- [3] Md. Mahiuddin Ahmed, A. Ranjitha Dhanasekaran, Aaron Block, Suhong Tong, Alberto C. S. Costa, Melissa Stasko, and Katheleen J. Gardiner. Protein dynamics associated with failed and rescued learning in the ts65dn mouse model of down syndrome. *PLOS ONE*, 10(3):1–25, 03 2015.
- [4] Philippe Boileau, Nima S Hejazi, and Sandrine Dudoit. Exploring high-dimensional biological data with sparse contrastive principal component analysis. *Bioinformatics*, 36(11):3422–3430, 03 2020.
- [5] Stephen Boyd, Stephen P Boyd, and Lieven Vandenberghe. *Convex optimization*. Cambridge university press, 2004.
- [6] Richard H Byrd, Peihuang Lu, Jorge Nocedal, and Ciyu Zhu. A limited memory algorithm for bound constrained optimization. *SIAM Journal on scientific computing*, 16(5):1190–1208, 1995.
- [7] Manuel G. Calvo and Daniel Lundqvist. Facial expressions of emotion (kdef): Identification under different display-duration conditions. *Behavior Research Methods*, 40(1):109–115, Feb 2008.
- [8] Pierre Comon. Independent component analysis, a new concept? *Signal Processing*, 36(3):287 – 314, 1994. Higher Order Statistics.
- [9] Dirk Eddelbuettel and Conrad Sanderson. Rcpparmadillo: Accelerating r with high-performance c++ linear algebra. *Computational Statistics and Data Analysis*, 71:1054–1063, March 2014.
- [10] J. H. Friedman and J. W. Tukey. A projection pursuit algorithm for exploratory data analysis. *IEEE Transactions on Computers*, C-23(9):881–890, 1974.
- [11] Karl Pearson F.R.S. Liii. on lines and planes of closest fit to systems of points in space. *The London, Edinburgh, and Dublin Philosophical Magazine and Journal of Science*, 2(11):559–572, 1901.
- [12] Benyamin Ghogh, Fakhri Karray, and Mark Crowley. Eigenvalue and generalized eigenvalue problems: Tutorial. *arXiv preprint arXiv:1903.11240*, 2019.
- [13] Gene Golub, Knut Solna, and Paul Van Dooren. Computing the svd of a general matrix product/quotient. *SIAM Journal on Matrix Analysis and Applications*, 22(1):1–19, 2000.

- [14] Clara Higuera, Katheleen J. Gardiner, and Krzysztof J. Cios. Self-organizing feature maps identify proteins critical to learning in a mouse model of down syndrome. *PLOS ONE*, 10(6):1–28, 06 2015.
- [15] Daniel D. Lee and H. Sebastian Seung. Learning the parts of objects by non-negative matrix factorization. *Nature*, 401(6755):788–791, Oct 1999.
- [16] Olaf Mersmann. *microbenchmark: Accurate Timing Functions*, 2019. R package version 1.4-7.
- [17] Yixuan Qiu and Jiali Mei. *RSpectra: Solvers for Large-Scale Eigenvalue and SVD Problems*, 2019. R package version 0.16-0.
- [18] R Core Team. *R: A Language and Environment for Statistical Computing*. R Foundation for Statistical Computing, Vienna, Austria, 2020.
- [19] Ronald Salloum and C.-C. Jay Kuo. Efficient image splicing localization via contrastive feature extraction. *CoRR*, abs/1901.07172, 2019.
- [20] Kristen A Severson, Soumya Ghosh, and Kenney Ng. Unsupervised learning with contrastive latent variable models. In *Proceedings of the AAAI Conference on Artificial Intelligence*, volume 33, pages 4862–4869, 2019.
- [21] Matthew Turk and Alex Pentland. Eigenfaces for recognition. *Journal of cognitive neuroscience*, 3(1):71–86, 1991.